Imaging Findings in Ulnar-sided Wrist Impaction Syndromes[1]

Luis Cerezal, MD • Francisco del Piñal, MD, PhD • Faustino Abascal, MD • Roberto García-Valtuille, MD • Teresa Pereda, MD • Ana Canga, MD

CME FEATURE

See accompanying test at http://www.rsna.org/education/rg_cme.html

LEARNING OBJECTIVES FOR TEST 5

After reading this article and taking the test, the reader will be able to:

- Describe the clinical manifestations of various ulnar-sided wrist impaction syndromes.
- Describe the imaging features of ulnar-sided wrist impaction syndromes and define the roles of current imaging modalities in the diagnosis of these entities.
- Provide a concise differential diagnosis and discuss appropriate treatment options for ulnar-sided wrist impaction syndromes.

Impaction syndromes related to ulnar-sided pain include ulnar impaction syndrome, ulnar impingement syndrome, ulnocarpal impaction syndrome secondary to nonunion of the ulnar styloid process, ulnar styloid impaction syndrome, and hamatolunate impingement syndrome. The most common of these, ulnar impaction syndrome, is a degenerative condition of the ulnar side of the wrist related to excessive load bearing across the ulnar carpus, triangular fibrocartilage (TFC) complex, and ulnar head. In an adequate clinical setting, characteristic osseous findings at radiography include positive ulnar variance in ulnar impaction syndrome, a short ulna in ulnar impingement syndrome, nonunion of the ulnar styloid process in ulnar impaction syndrome secondary to ulnar styloid nonunion, an excessively long ulnar styloid process in ulnar styloid impaction syndrome, and type II lunate bone in hamatolunate impingement syndrome. Nevertheless, confirmation of clinical and conventional radiographic findings with magnetic resonance (MR) imaging is often necessary to exclude other entities with similar clinical manifestations. MR imaging allows earlier detection of an abnormality in the TFC complex, cartilage, or bone marrow of carpal bones and is helpful in formulating the extensive differential diagnosis in patients with ulnar wrist pain and limitation of motion.

Abbreviations: TFC = triangular fibrocartilage, USPI = ulnar styloid process index

Index terms: Wrist, fractures, 43.41 • Wrist, injuries, 43.41, 43.432, 43.483 • Wrist, MR, 43.1214 • Wrist, radiography, 43.11

RadioGraphics 2002; 22:105–121

[1]From the Department of Radiology, Instituto Radiológico Cántabro, Clínica Mompía, Mompía, 39100 Cantabria, Spain (L.C., F.A., R.G.V., T.P., A.C.); and the Private Hand-Wrist and Plastic-Reconstructive Surgery and Hand Surgery Department, Mutua Montañesa, Rualasal, Santander, Spain (F.d.P.). Recipient of a Cum Laude award for an education exhibit at the 2000 RSNA scientific assembly. Received April 19, 2001; revision requested May 17 and received June 25; accepted July 2. **Address correspondence to** L.C. (e-mail: *lcerezal@mundivia.es*).

a. b.

c.

Figure 1. Ulnar variance. The degree of variance is determined by projecting a line perpendicular from the carpal joint surface of the distal end of the radius toward the ulna and measuring the distance in millimeters between this line and the carpal surface of the ulna. Conventional posteroanterior radiographs of the wrist in neutral deviation show positive ulnar variance with the articular surface of the ulna projecting distal to the articular surface of the radius **(a)**, neutral variance with equal length of the radial articular surfaces of the radius and ulna **(b)**, and negative variance with the distal edge of the ulna proximal to the distal articular surface of the radius **(c)**.

Introduction

Ulnar wrist pain has historically been a diagnostic challenge for radiologists and hand surgeons. The medical literature of the past 2 decades is replete with articles discussing ulnar-sided wrist pain centered on the triangular fibrocartilage (TFC) complex. This heightened interest has resulted in clinical data that have improved the understanding of the anatomy, biomechanics, and pathologic conditions of the distal radioulnar joint and ulnar carpus. However, diagnosis remains difficult and is often delayed because significant disease and incapacitating pain may be present in spite of minimal evidence at conventional radiography.

There are a variety of impaction syndromes associated with ulnar-sided wrist pain. The most common of these syndromes is ulnar impaction syndrome, a well-recognized and relatively frequent source of ulnar wrist pain and limitation of motion (1–4). In this article, we review the concept of ulnar variance and discuss and illustrate the spectrum of imaging findings and differential diagnoses in ulnar impaction syndrome. We also review the imaging findings in other, less common ulnar-sided impaction syndromes, including ulnar impingement syndrome, ulnocarpal impaction syndrome secondary to nonunion of the ulnar styloid process, ulnar styloid impaction syndrome, and hamatolunate impingement syndrome.

a. b.

Figure 2. Effect of gripping on ulnar variance. **(a)** Conventional posteroanterior radiograph of the wrist in neutral deviation shows slightly positive ulnar variance (line). **(b)** Radiograph obtained during forearm pronation combined with a firm grip shows a significant increase in ulnar variance (line).

Ulnar Variance

The term *ulnar variance*, or radioulnar index, refers to the relative lengths of the distal articular surfaces of the radius and ulna. This is usually referred to as Hulten variance and may be neutral (both articular surfaces the same length), positive (ulnar surface longer), or negative (ulnar surface shorter) (Fig 1) (5). Variance is independent of the length of the ulnar styloid process, which may also vary. However, wrist position is an important determinant of ulnar variance (2,6–9). Maximum forearm pronation results in an increase in positive ulnar variance, whereas maximum forearm supination decreases ulnar variance. Ulnar variance increases significantly with a firm grip and returns to its original state with cessation of grip. The magnitude of change varies considerably but is generally in the range of 1–2 mm. Ulnar variance is not a constant and can be affected by daily activities that involve repetitive forearm rotation and gripping (2,6–9). Clearly, a standard radiographic view is necessary to help reliably determine ulnar variance. The generally accepted standard view is a posteroanterior view obtained with the wrist in neutral forearm rotation, the elbow flexed 90°, and the shoulder abducted 90°. This positioning provides an image of the radioulnar length with the wrist unloaded (7,10). However, such a view may underestimate variance in wrists in which a firm grip and pronation result in significant proximal migration of the radius (Fig 2). Therefore, preoperative ulnar variance should be measured on radiographs obtained during neutral forearm rotation and during forearm pronation combined with a firm grip before selecting a treatment for causes of ulnar wrist pain that are affected by radioulnar length (1). Although magnetic resonance (MR) imaging can help estimate the degree of ulnar variance, making direct ulnar variance measurements on standard wrist MR images is not appropriate. The specific position required to determine ulnar variance usually cannot be duplicated at MR imaging, and the image interpreter must exercise caution in describing subtle ulnar variance on MR images of the wrist.

Palmer Classification Scheme for TFC Complex Lesions

Class or Subclass	Description
I	Traumatic injury
IA	Central perforations
IB	Ulnar avulsion with or without distal ulnar fracture
IC	Distal avulsion (carpal attachment)
ID	Radial avulsion with or without sigmoid notch fracture
II	Degenerative injury
IIA	TFC complex wear
IIB	TFC complex wear, lunate or ulnar chondromalacia
IIC	TFC complex perforation, lunate or ulnar chondromalacia
IID	TFC complex perforation, lunate or ulnar chondromalacia, lunotriquetral ligament perforation
IIE	TFC complex perforation, lunate or ulnar chondromalacia, lunotriquetral ligament perforation, ulnocarpal osteoarthritis

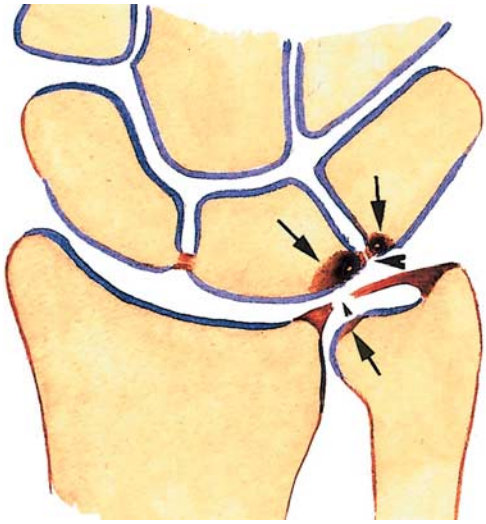

Figure 3. Diagram illustrates the full spectrum of pathologic conditions in ulnar impaction syndrome, including chondromalacia of the ulnar head, the ulnar side of the lunate bone, and the radial side of the triquetral bone (arrows); central perforation of the TFC (small arrowhead); and lunotriquetral ligament tear (large arrowhead).

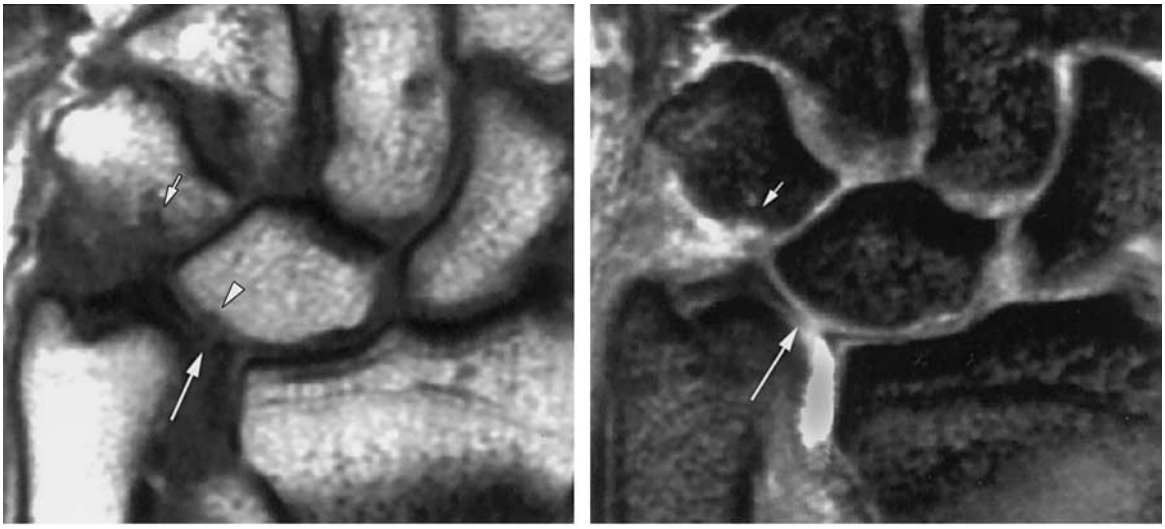

a. **b.**

Figure 4. Ulnar impaction syndrome in a 32-year-old woman with significant positive variance and insidious onset of ulnar-sided pain (Palmer class IIC lesion). Coronal T1-weighted (repetition time msec/echo time msec = 500/15) **(a)** and gradient-echo (400/18, 20° flip angle) **(b)** MR images show marked positive ulnar variance, central perforation of the TFC (long arrow), and chondromalacia of the lunate bone (arrowhead in **a**) and triquetral bone (short arrow). An arthroscopic "wafer" procedure was performed, with excellent results.

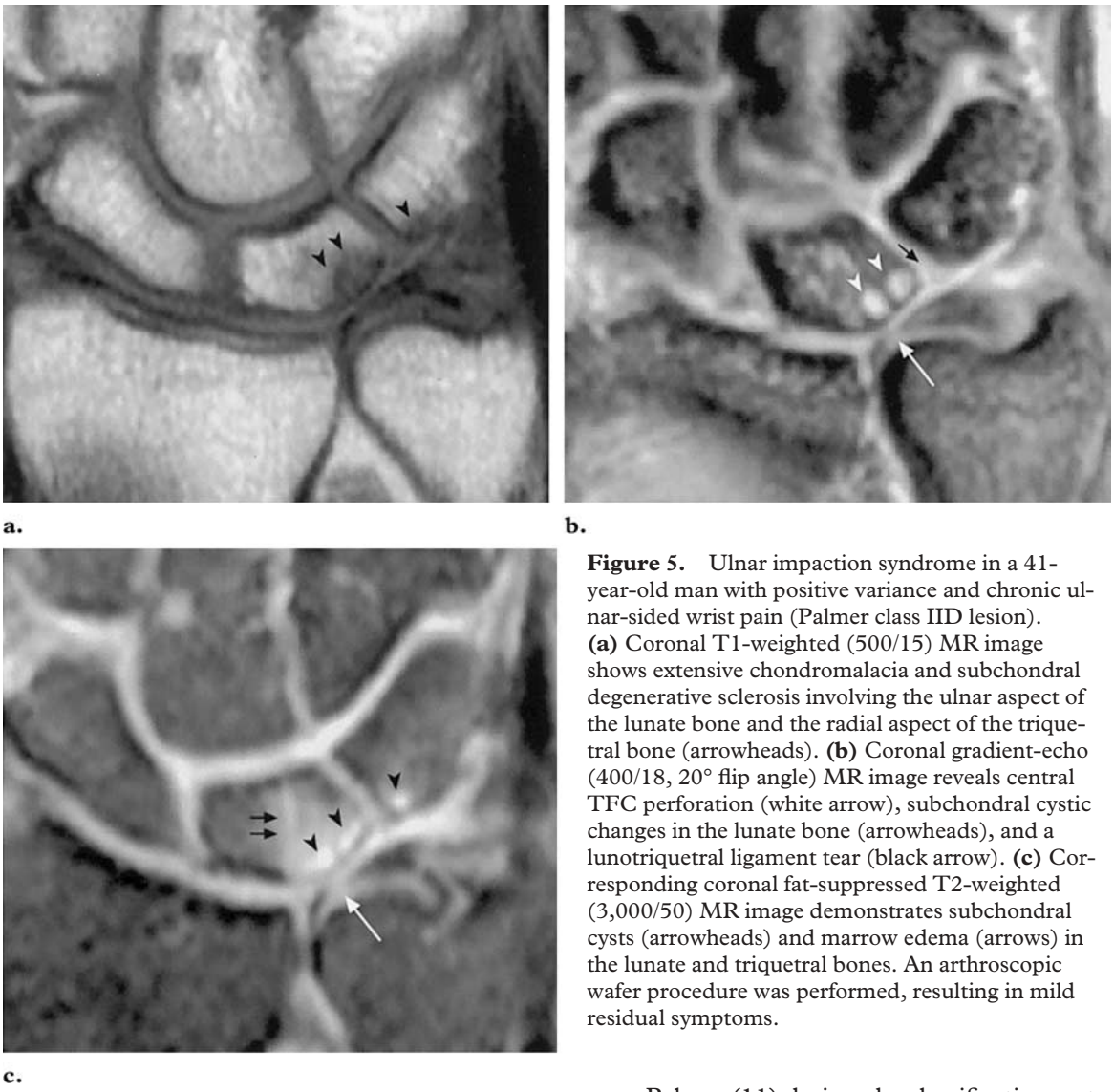

Figure 5. Ulnar impaction syndrome in a 41-year-old man with positive variance and chronic ulnar-sided wrist pain (Palmer class IID lesion). **(a)** Coronal T1-weighted (500/15) MR image shows extensive chondromalacia and subchondral degenerative sclerosis involving the ulnar aspect of the lunate bone and the radial aspect of the triquetral bone (arrowheads). **(b)** Coronal gradient-echo (400/18, 20° flip angle) MR image reveals central TFC perforation (white arrow), subchondral cystic changes in the lunate bone (arrowheads), and a lunotriquetral ligament tear (black arrow). **(c)** Corresponding coronal fat-suppressed T2-weighted (3,000/50) MR image demonstrates subchondral cysts (arrowheads) and marrow edema (arrows) in the lunate and triquetral bones. An arthroscopic wafer procedure was performed, resulting in mild residual symptoms.

Ulnar Impaction Syndrome

Ulnar impaction syndrome, also known as ulnar abutment or ulnocarpal loading, is a degenerative condition characterized by ulnar wrist pain, swelling, and limitation of motion related to excessive load bearing across the ulnar aspect of the wrist. Chronic impaction between the ulnar head and the TFC complex and ulnar carpus results in a continuum of pathologic changes (Fig 3): degenerative tear of the TFC; chondromalacia of the lunate bone, triquetral bone, and distal ulnar head; instability or tear of the lunotriquetral ligament; and, finally, osteoarthritis of the ulnocarpal and distal radioulnar joints (1–4).

Palmer (11) designed a classification system for TFC complex lesions based on mechanism, location, and involved structures (Table). This classification system is helpful in determining the mechanism of injury and directing clinical management. It divides lesions into two classes. Class I (traumatic) lesions are subclassified according to the site of TFC complex involvement. Class II (degenerative) lesions demonstrate the entire spectrum of findings in ulnar impaction syndrome and are subclassified according to the degree of involvement of structures on the ulnar side of the wrist, highlighting the progressive nature of these injuries (Figs 4, 5) (12).

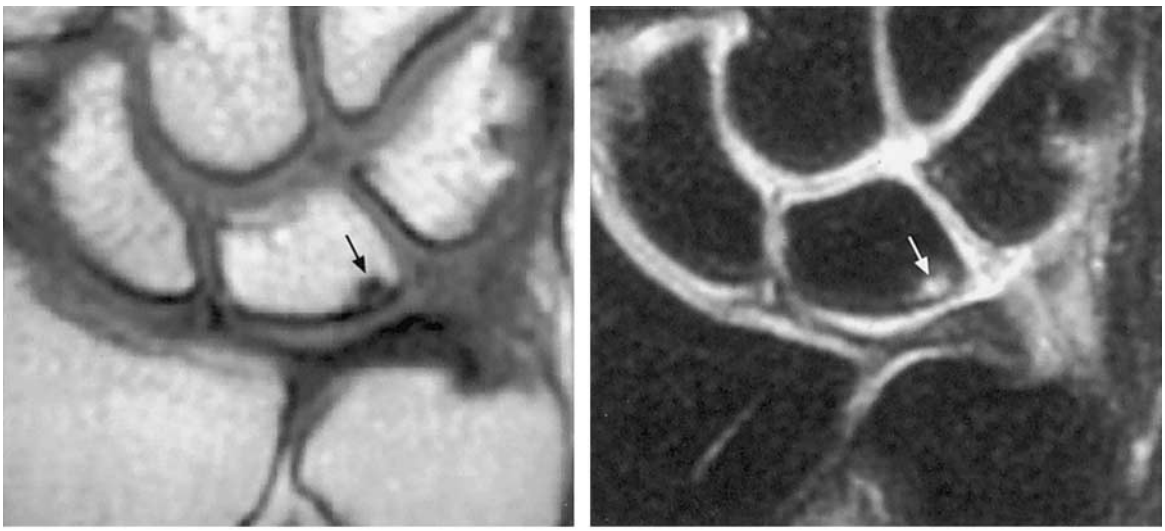

a. b.

Figure 6. Ulnar impaction syndrome in a 24-year-old man with neutral variance and ulnar-sided wrist pain. **(a)** Coronal T1-weighted (500/15) MR image demonstrates a small focus of low signal intensity in the subchondral ulnar corner of the lunate bone (arrow). **(b)** Corresponding coronal fat-suppressed T2-weighted (3,000/50) MR image shows focal loss of lunate articular cartilage and high-signal-intensity marrow edema within the corresponding area of the lunate bone (arrow). The TFC complex is intact. An arthroscopic wafer procedure was performed, resulting in complete resolution of symptoms.

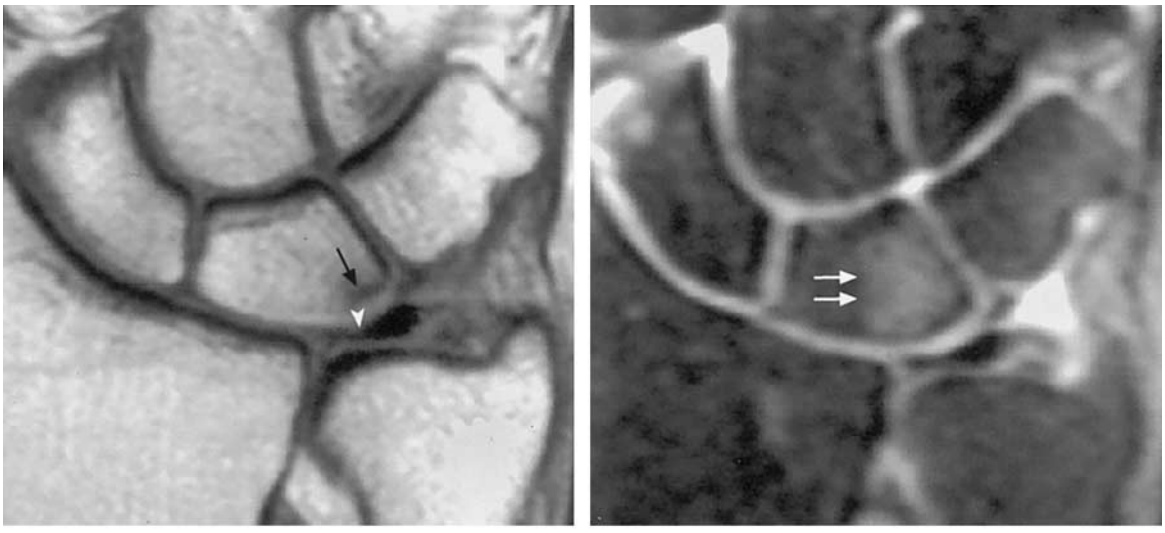

a. b.

Figure 7. Ulnar impaction syndrome in a 34-year-old woman with negative ulnar variance. Coronal T1-weighted (500/15) **(a)** and corresponding fat-suppressed T2-weighted (3,000/50) **(b)** MR images clearly depict chondromalacia and marrow edema of the lunate bone (arrows). The TFC is slightly thinned and frayed (arrowhead in **a**). Ulnar shortening was performed, with excellent results.

The pathologic changes that appear in ulnar impaction syndrome most commonly occur with positive ulnar variance but can occasionally occur with neutral or negative ulnar variance (Figs 6, 7) (1,13). The most common predisposing factors include congenital positive ulnar variance, malunion of the distal radius (Fig 8), premature physeal closure of the distal radius, and previous radial head resection (1). The latter is occasionally performed after an unrecognized Essex-Lopresti

Figure 8. Ulnar impaction syndrome secondary to fracture of the distal radius in a 59-year-old woman. Posteroanterior radiograph of the right wrist shows an old fracture of the distal radius with secondary radial shortening. Subcortical sclerosis is present along the ulnar aspect of the proximal pole of the lunate bone (arrow).

fracture-dislocation, which is a massive axial radioulnar derangement consisting of disruption of the distal radioulnar joint, rupture of the interosseous membrane, and impaction fracture of the radial head. All of these predisposing factors result in a fixed increase in underlying ulnar loading associated with relative lengthening of the ulna or increased dorsal tilt of the distal radius (1,4). In the absence of obvious structural abnormalities, ulnar impaction syndrome may result from daily activities that cause excessive intermittent loading of the ulnar carpus (1,4,13). It has also been shown that asymptomatic changes in ulnocarpal impaction syndrome develop over time, so that this condition may be present even if symptoms are not evident.

The clinical manifestation of ulnar impaction syndrome generally consists of chronic or subacute ulnar wrist pain, often exacerbated by activity and relieved by rest. Swelling and limitation of forearm rotation and wrist motion are frequent concurrent complaints. Anything that causes a relative increase in ulnar variance (eg, firm grip, pronation, ulnar deviation of the wrist) exacerbates the symptoms (1,4).

Radiographic findings in ulnar impaction syndrome include positive ulnar variance and, less frequently, neutral or negative variance. Underlying abnormalities, including malunion of a distal radial fracture with residual radial shortening and abnormal dorsal tilt, may be present. Premature physeal arrest of the distal radius or previous Essex-Lopresti fracture or resection of the radial head may also be evident on conventional radiographs. Secondary changes in the ulnar carpus include subchondral sclerosis and cystic changes in the ulnar head, ulnar aspect of the proximal lunate bone, and proximal radial aspect of the triquetral bone (1,2,4). In more advanced disease, ulnocarpal osteoarthritis may be seen in these same areas. Although the radiographic changes may be striking, the features of ulnar impaction syndrome may be subtle in both its early and late stages. In such cases, recognition of the geographic nature of the abnormalities affecting the articular surfaces of the ulna, lunate bone, and triquetral bone is paramount for making the correct diagnosis (1,2,4). In the setting of negative or questionable negative conventional radiographs and a strong clinical suspicion for ulnar impaction, MR imaging is helpful in detecting occult disease (1,3). In the early stage of ulnar impaction syndrome, the joint cartilage of the ulnar head and ulnar carpus is characterized by fibrillation. Progression of the syndrome results in bone hyperemia, which has low signal intensity on T1-weighted images and high signal intensity on T2-weighted images. Further progression results in sclerotic changes, which appear as areas of low signal intensity on both T1- and T2-weighted images. In patients with radiographic evidence of ulnar impaction syndrome, wrist MR imaging and MR arthrography may be necessary to demonstrate the integrity of the TFC and lunotriquetral ligament (1,3,4).

The differential diagnosis must include asymptomatic senescent changes, intraosseous ganglia, true cysts, vascular grooves, and Kienböck disease. The distribution of radiographic changes within the lunate bone is the key to distinguishing these conditions from ulnar impaction (3,4). Intraosseous ganglia and true cysts appear on conventional radiographs as a radial-sided area of hyperlucency that communicates with the scapholunate joint space or a hyperlucent area within the distal ulnar aspect of the lunate bone that communicates with the lunotriquetral joint space. Intraosseous ganglia and true cysts both demonstrate low signal intensity on T1-weighted

MR images and high signal intensity on T2-weighted images, similar to water. Differentiation is aided by a lack of clinical findings, sharper margins seen on radiographs, and a lack of changes in signal intensity in the triquetral bone or ulnar head (3,4). Senescent changes are best differentiated by (*a*) a lack of positive ulnar variance and (*b*) local tenderness over the ulnar carpus, ulnar head, or both (3). A vascular groove usually appears as a central proximal radiolucent defect that communicates with the radiolunate joint space (4). The signal intensity pattern in Kienböck disease may mimic that in ulnar impaction syndrome; however, Kienböck disease lesions are more diffuse or affect the radial half of the lunate bone compared with involvement of only the ulnar aspect in ulnar impaction syndrome. Furthermore, the triquetral bone and the ulnar head are not affected in Kienböck disease (3,4).

Treatment of symptomatic ulnar impaction is complex in that it varies with the amount of ulnar variance, the Palmer lesion class, the shape of the sigmoid fossa and ulnar seat (14–18), and the presence of concomitant lunotriquetral instability. Briefly, Palmer class IIA and IIB lesions (no TFC perforation) are managed with an open wafer procedure (13,19), which consists of surgical resection of the distalmost 2–3 mm of the dome of the ulnar head or formal ulnar shortening (ie, excision of a slice [generally 2–3 mm wide] of the ulnar shaft followed by rigid fixation) (1,17). When the TFC is already perforated (Palmer class IIC and IID lesions), the head of the ulna can be burred down with the help of arthroscopic instrumentation (arthroscopic wafer procedure). This procedure is minimally invasive, highly effective, and allows rapid return to normal activities (20); in fact, some authors currently consider it optimal to perforate the TFC in class IIA and IIB lesions and then perform an arthroscopic wafer procedure as one would in IIC and IID lesions (20). Class IIE lesions are managed with salvage procedures such as complete or partial ulnar head resection (Darrach procedure and similar procedures) or arthrodesis of the distal radioulnar joint with distal ulnar pseudoarthrosis (Sauvé-Kapandji procedure). Unfortunately, none of these procedures is ideal because they all produce convergent instability (discussed later). Ulnar impaction secondary to an Essex-Lopresti fracture-dislocation deserves separate consideration because successful treatment is not possible in the chronic setting (21,22). Ulnar shortening in particular is doomed to failure because the ruptured interosseous membrane allows the radial column to recede until the proximal radial metaphysis impacts against the capitellum. Thus, it is vital to consider the feasibility of an Essex-Lopresti injury in any impaction fracture of the radial head in the acute setting. This will allow appropriate management of the full injury and not just of the radial head fracture.

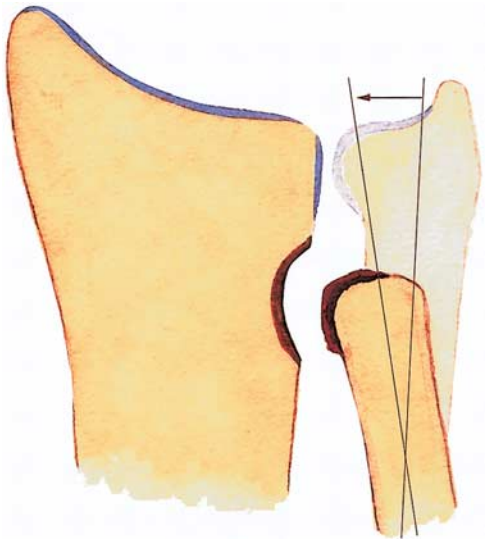

Figure 9. Diagram illustrates the three cardinal features of ulnar impingement syndrome secondary to distal ulnar resection: a shortened ulna proximal to the sigmoid notch, scalloping of the distal radius, and radioulnar convergence (arrow).

Ulnar Impingement Syndrome

Although the literature frequently uses the terms *ulnar impingement* and *ulnar impaction* interchangeably, these entities are not only distinct but mutually exclusive. Ulnar impingement syndrome is caused by a shortened distal ulna that impinges on the distal radius proximal to the sigmoid notch (23,24). The clinical manifestation of ulnar im-

a. b.

Figure 10. Ulnar impingement in a 72-year-old woman with advanced rheumatoid arthritis. The patient had experienced distal forearm pain since undergoing the Darrach procedure 5 years earlier. **(a)** Posteroanterior radiograph obtained with the patient in the resting position shows extensive distal ulnar excision, focal remodeling and sclerosis of the distal radius (arrowheads), and proliferative changes in the distal ulnar stump and distal radius (arrow). **(b)** Posteroanterior radiograph obtained during maximum grip shows contact between the distal ulnar stump and the distal radius (dynamic radioulnar convergence).

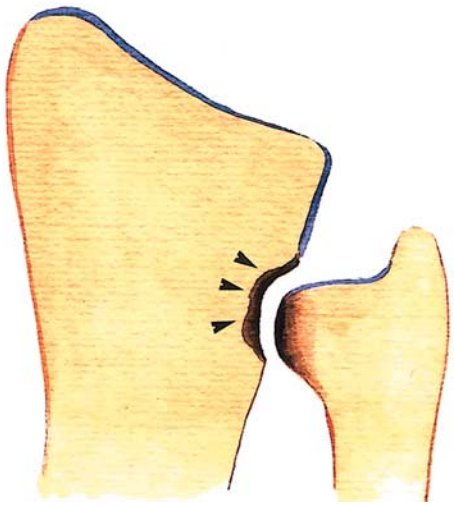

Figure 11. Diagram illustrates ulnar impingement secondary to significant negative ulnar variance or premature fusion of the distal ulna. Note the scalloping of the distal radius proximal to the sigmoid notch (arrowheads).

pingement syndrome can be similar to that of ulnar impaction syndrome; however, patients with ulnar impingement syndrome will generally experience a great deal of discomfort on pronation and supination of the forearm. Compression of the distal radioulnar joint on forearm rotation increases the symptoms or produces grating in affected patients and is very useful in identifying incongruity of the distal radioulnar joint (1,4,23–25). Most often, a markedly shortened distal ulna results from any of the surgical procedures that involve resection of the distal ulna secondary to prior wrist trauma, rheumatoid arthritis, or correction of Madelung deformity (Figs 9, 10) (23). Less commonly, ulnar impingement may be present in de novo cases of negative ulnar variance or premature fusion of the distal ulna secondary to prior trauma (Figs 11, 12) (4,23).

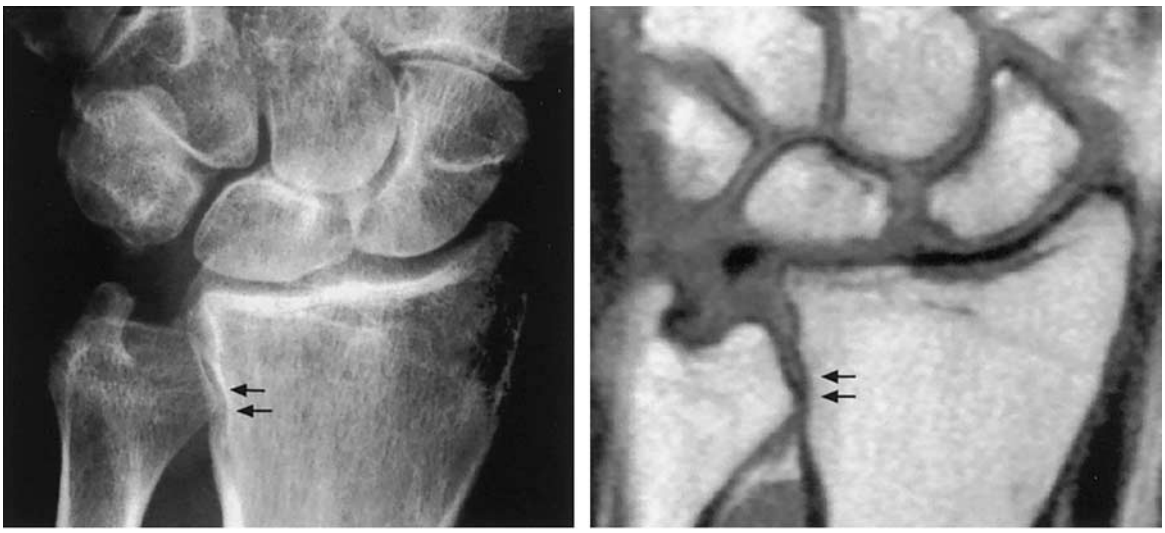

a. b.

Figure 12. Ulnar impingement in a 22-year-old man with chronic wrist pain. **(a)** Posteroanterior radiograph of the left wrist shows prominent ulnar shortening, scalloping, and sclerosis along the ulnar margin of the distal radius proximal to the sigmoid notch (arrows). **(b, c)** Coronal T1-weighted (500/15) **(b)** and gradient-echo T2-weighted (400/18, 20° flip angle) **(c)** MR images demonstrate negative ulnar variance and characteristic radial remodeling (arrows). Note the secondary deformity of the TFC (arrowhead in **c**).

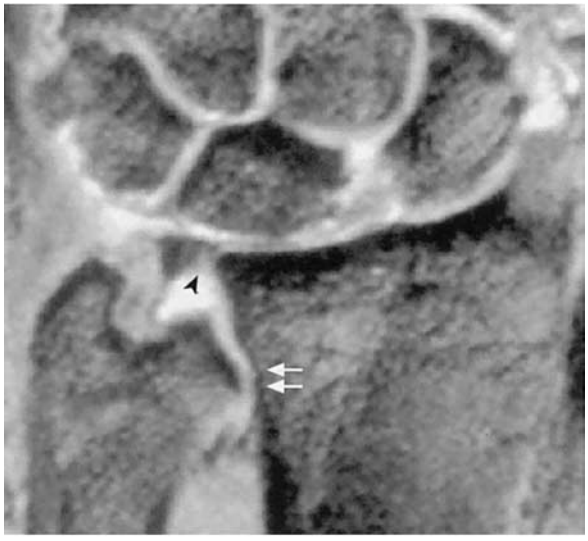

c.

When the distal ulna is shortened for whatever reason, the contraction of the extensor pollicis brevis, abductor pollicis longus, and pronator quadratus muscles and the effect of the interosseous membrane with the loss of the buttress effect of the radioulnar joint cause approximation of the lower ends of the radius and ulna (23,24). This is known as radioulnar convergence and is rarely symptomatic, in contrast to ulnar impingement syndrome, in which distal radioulnar contact is evident and causes pain (23,24).

Ulnar impingement can produce erosive cortical changes at the corresponding level of the radius that appear as scalloping on conventional radiographs (24,25). By the time such changes are seen, the condition has been present for many years. The presence of subchondral sclerosis, the stress-loaded radiologic view described by Lees and Scheker (25), and MR imaging are all helpful in confirming the diagnosis before such erosive changes are visible. They also increase the possibility of earlier recognition of this condition.

Although convergence is quite common after the Darrach procedure and similar procedures, symptomatic ulnar impingement is rare (24)—which is fortunate, because fully successful treatment does not yet exist. Aggressive ulnar shortening has been proposed (26), but the procedure has not yet stood the test of time. One of the authors (F.d.P.) successfully treated a patient with rheumatoid arthritis at 7 years follow-up by resecting all osteophytes, shortening the ulna by 1 cm, wrapping the stump with a tendon graft, and stabilizing the stump with tenodesis of the extensor carpi ulnaris tendon. Perhaps the definitive answer lies in ulnar head prostheses (27,28), which presently are not appropriate for patients who would place high demands on them. The

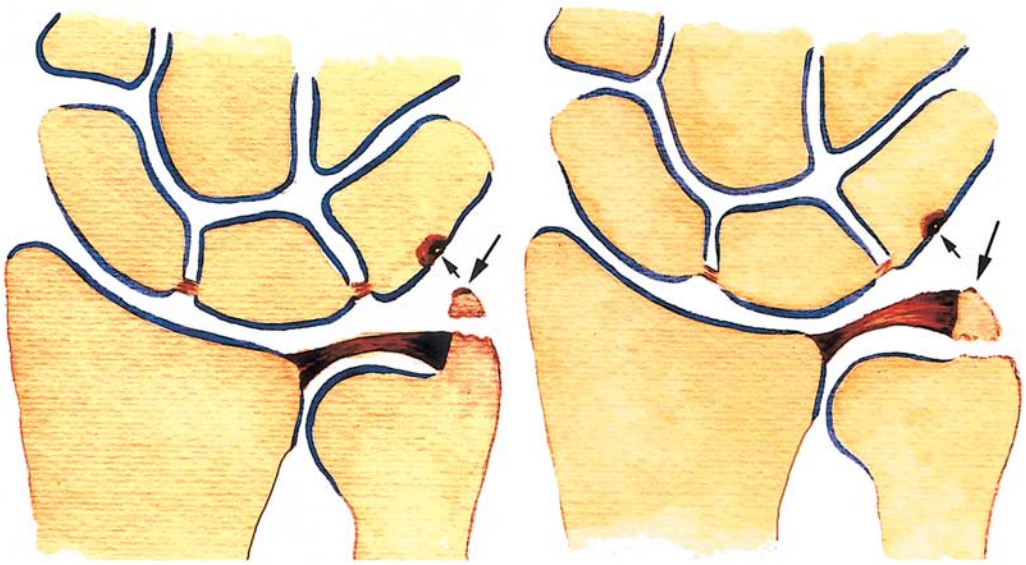

Figure 13. **(a)** Diagram illustrates type 1 ulnar styloid nonunion, with the TFC complex and distal radioulnar joint stability intact. **(b)** Diagram illustrates type 2 ulnar styloid nonunion, with avulsion of the ulnar attachment of the TFC complex (Palmer class IB lesion) and secondary instability of the distal radioulnar joint. Both diagrams illustrate how the nonunited fragment acts as an irritative loose body, causing focal chondromalacia of the triquetral bone (short arrow) and subcortical sclerosis on the tip of the fragment (long arrow).

approach is totally different when convergence is due to a severely shortened ulna caused by a growing defect because distraction lengthening of the ulna can restore the normal anatomy (29). With the application of Scheker's principles for treatment of early distal radioulnar joint osteoarthritis (30), less marked ulnar shortness might benefit from radial shortening performed in an attempt to change the contact area between the ulnar head and the sigmoid notch (30). Finally, in the setting of ulnar shortness, consideration should be given to generalized wrist disorders such as minor forms of ulnar club hand because isolated lengthening of the ulna will not be successful in these cases (31).

Ulnocarpal Impaction Syndrome Secondary to Ulnar Styloid Nonunion

Fractures of the ulnar styloid process can occur as isolated injuries or, more commonly, in association with fractures of the distal radius (10,32–34). Ulnar styloid nonunion is not uncommon following a fracture (32). Symptomatic nonunion of the ulnar styloid process is probably underrecognized or underreported in the literature (10,34). Nonunion of the ulnar styloid process may become symptomatic for different reasons (34). The nonunited fragment may act as an irritative loose body or abut the ulnar carpus. A malaligned fibrous nonunion may cause impingement of the extensor carpi ulnaris tendon sheath. Such a nonunion may also be symptomatic because of associated TFC complex perforation or may be associated with complete rupture of the ulnar attachments of the TFC complex and instability of the distal radioulnar joint. Any of these conditions alone or in combination may be responsible for painful ulnar styloid nonunion (34). Two types of nonunion of the ulnar styloid process have been described in terms of anatomic features and treatment options (34). Type 1 is defined as a nonunion associated with a stable distal radioulnar joint. It affects only the tip of the styloid process, and the TFC complex remains intact because its major attachments are at the base of the styloid process, so that the distal radioulnar joint remains stable (Fig 13a). Type 2 is defined as a nonunion

a. b.

Figure 14. Ulnocarpal impaction syndrome secondary to nonunion of the ulnar styloid process in a 26-year-old man with insidious ulnar-sided pain. Coronal T1-weighted (500/15) **(a)** and fat-suppressed T2-weighted (3,000/50) **(b)** MR images reveal nonunion of the ulnar styloid process (white arrow) associated with ulnar avulsion of the TFC complex (Palmer class IB TFC complex injury) (arrowhead in **b**) and early chondromalacia of the triquetral bone with subchondral edema (black arrow). Results of arthroscopic examination confirmed early focal chondromalacia of the triquetral bone. The patient underwent excision of the fragment and repair of the TFC complex, with excellent results.

associated with subluxation of the distal radioulnar joint. It is the result of an avulsion of the ulnar attachment of the TFC complex (Palmer class IB lesion) (Fig 13b).

MR imaging is an excellent modality for visualizing the integrity of the TFC complex and its ulnar attachments, the presence of nonunited bone fragments, and associated chondromalacia of the ulnar carpus (Fig 14). Accessory ossicles in these anatomic regions such as the lunula and os triangulare may be confused with nonunion of the ulnar styloid process. They often occur bilaterally without evidence of trauma. Whether their origin is a detached ossification center for the ulnar styloid process, ossification of normal soft tissue, or a nonunited fracture of the ulnar styloid process, no further work-up or therapy is necessary if the wrist is asymptomatic (34). Surgical treatment should be preceded by diagnostic arthroscopy, which allows the condition to be classified as one of the subtypes mentioned earlier. At palpation with an arthroscopic probe, the TFC complex is normally resilient centrally, and at ballottement with the probe, this central portion bounces like an athlete on a trampoline (35). If the TFC complex has lost its resiliency and shows lack of the normal "trampoline effect," the ulna styloid process (along with the TFC complex) should be reinserted in the fovea and appropriately fixed by means of a limited incision in the ulnar aspect of the wrist (34). This will mean a major derangement of the ulnar insertion of the TFC complex (type 2 nonunion). Conversely, if the TFC complex demonstrates the normal trampoline effect (ie, is resilient during probing), the offending bone fragment should be removed—at arthroscopy, if possible—and the full range of motion immediately established because the stability of the distal radioulnar joint will not be affected.

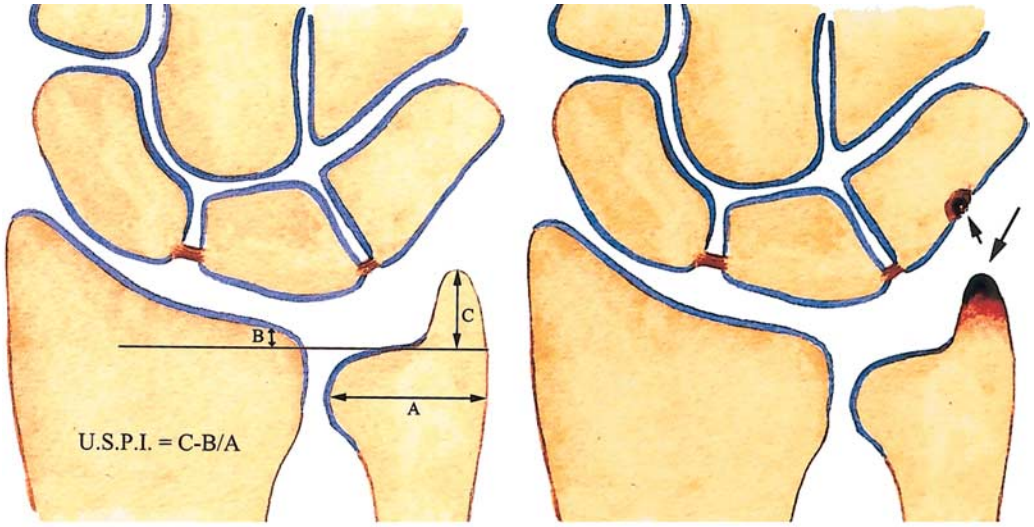

15. 16.

Figures 15, 16. **(15)** Diagram (coronal view) illustrates the USPI, which is calculated by subtracting the degree of ulnar variance (*B*) from the length of the ulnar styloid process (*C*) and dividing the difference by the transverse diameter of the ulnar head (*A*). The USPI has a normal range of 0.21 ± 0.07. **(16)** Diagram (coronal view) illustrates the pathologic conditions that characterize ulnar styloid impaction syndrome, including chondromalacia of the proximal pole of the triquetral bone (short arrow) and subcortical sclerosis on the styloid process (long arrow).

Ulnar Styloid Impaction Syndrome

Ulnar styloid impaction syndrome is distinctly different from the more well known form of ulnar impaction syndrome in that the radiographic evidence of chondromalacia does not involve the proximal pole of the lunate bone and ulnar head, but rather the proximal pole of the triquetral bone and the ulnar styloid process. This ulnar-sided wrist pain is caused by impaction between an excessively long ulnar styloid process and the triquetral bone (36). The ulnar styloid process is a continuation of the prominent subcutaneous ridge of the shaft of the ulna, which projects distally toward the triquetral bone for a variable distance (2–6 mm) (37). Garcia-Elias (38) has developed a method of assessing the relative size of the process called the ulnar styloid process index (USPI) (Fig 15). An excessively long ulnar styloid process has a USPI greater than 0.21 ± 0.07 or an overall length greater than 6 mm (38).

Topper et al (36) have suggested the presence of a pathologic sequence of events in patients with an excessively long ulnar styloid process. One-time or repetitive impaction between the tip of the ulnar styloid process and the triquetral bone results in contusion, which leads to chondromalacia of the opposing articular surfaces (Fig 16), synovitis, and pain. If a single-event trauma is forceful enough, fracture of the dorsal triquetral bone may occur (38,39). Impaction over a long period of time can lead to lunotriquetral instability (36). The diagnosis of this condition is made on the basis of radiographic evidence of an excessively long ulnar styloid process in combination with positive findings on a provocative clinical test as described by Ruby (36). MR imaging may show

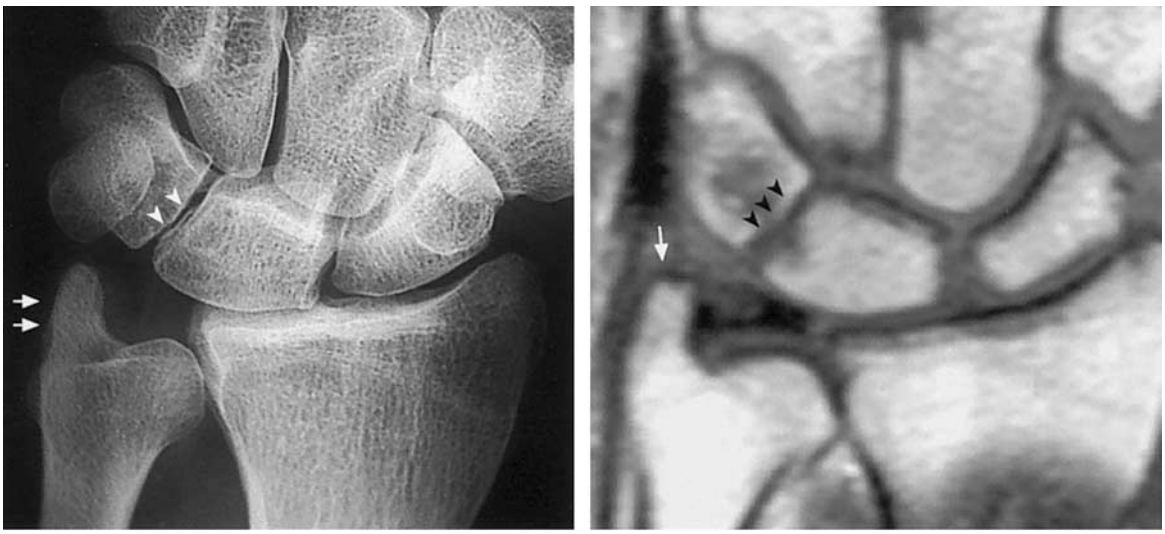

a. b.

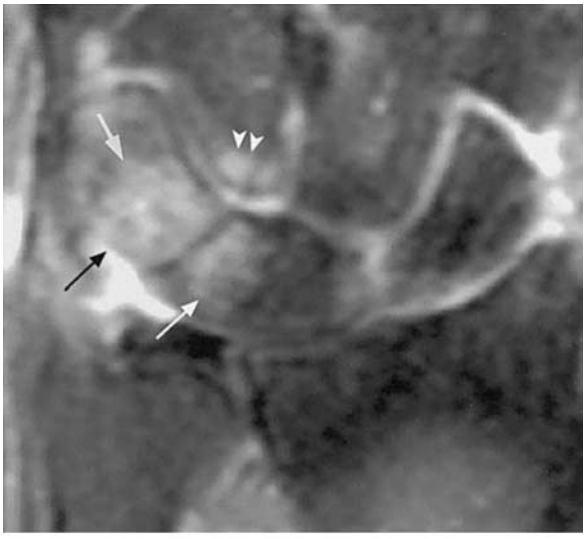

c.

Figure 17. Ulnar styloid impaction syndrome in a 44-year-old man with severe chronic ulnar-sided pain. **(a)** Posteroanterior radiograph shows an excessively long ulnar styloid process (arrows) and degenerative changes in the lunotriquetral joint with space narrowing (arrowheads). **(b)** Coronal T1-weighted (500/15) MR image reveals focal subchondral sclerosis on the tip of the styloid process (arrow) and advanced degenerative changes in the lunotriquetral joint (arrowheads). **(c)** Corresponding coronal fat-suppressed T2-weighted (3,000/50) MR image shows extensive chondromalacia of the triquetral bone (black arrow), degenerative changes in the lunotriquetral joint with extensive subchondral edema (white arrows), and chondromalacia of the hamate bone (arrowheads). Resection of the two most distal millimeters of the styloid process was performed, resulting in good recovery of function but mild residual ulnar wrist pain.

chondromalacia of the ulnar styloid process and proximal triquetral bone (Fig 17).

Resection of all but the two most proximal millimeters of the styloid process (so as not to interfere with the TFC complex insertion) is the treatment of choice (36).

Hamatolunate Impaction Syndrome

Hamatolunate impingement is an uncommon cause of ulnar-sided wrist pain that has been described recently (17,40). The characteristic ana-

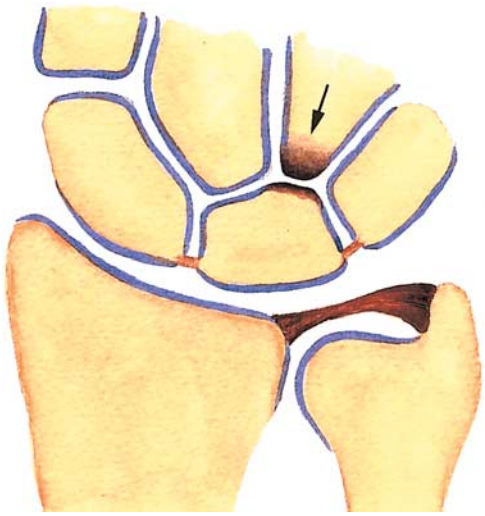

Figure 18. Diagram illustrates hamatolunate impaction syndrome, with Viegas type II lunate bone, chondromalacia of the proximal pole of the hamate bone, subchondral sclerosis, and marrow edema (arrow).

Figure 19. Hamatolunate impaction syndrome in a 36-year-old man. **(a)** Posteroanterior radiograph of the wrist in full ulnar deviation shows abutment of the hamate and lunate bones (arrow). **(b, c)** Coronal T1-weighted (500/15) **(b)** and fat-suppressed T2-weighted (3,000/50) **(c)** MR images show type II lunate bone with adjacent marrow edema of the hamate bone (arrow) and severe chondromalacia of the hamate bone, a finding that was proved at arthroscopy. Note the linear defect in the proximal aspect of the lunate bone (arrowhead), a finding that suggests a vascular groove.

tomic variant, consisting of an articulation between the hamate bone and the lunate bone (type II lunate bone) and described by Viegas et al (41), leads to a higher prevalence of chondromalacia of the proximal pole of the hamate bone (Fig 18) than in wrists without this articulation (type I lunate bone) (41–43). The repeated impingement and abrasion of these two bones when the wrist is used in full ulnar deviation (Fig 19a) is the suggested mechanism for the development of the chondromalacia (40,44). It has been reported that approximately 50% of lunate bones have a separate medial facet on the distal surface for articulation with the hamate bone; in about one-fourth of these cases, there is erosion of the cartilage with exposed subchondral bone on the proximal pole of the hamate bone (Fig 19), which is often occult at MR imaging (45).

Arthroscopic burring of the apex of the hamate bone through a midcarpal portal represents the state-of-the-art treatment of this condition (17, 40). Short-term results are very encouraging, although long-term follow-up is still lacking.

Conclusions

The differential diagnosis in patients with ulnar wrist pain and limitation of motion is extensive. MR imaging is an excellent modality for visualizing the full spectrum of abnormalities in ulnar-sided wrist impaction syndromes. Confirmation

of clinical and conventional radiographic findings with MR imaging is often necessary to exclude other entities with similar clinical manifestations.

References

1. Friedman SL, Palmer AK. The ulnar impaction syndrome. Hand Clin 1991; 7:295–310.
2. Escobedo EM, Bergman AG, Hunter JC. MR imaging of ulnar impaction. Skeletal Radiol 1995; 24:85–90.
3. Imaeda T, Nakamura R, Shionoya K, Makino N. Ulnar impaction syndrome: MR imaging findings. Radiology 1996; 201:495–500.
4. Hodge JC, Yin Y, Gilula LA. Miscellaneous conditions of the wrist. In: Gilula LA, Yin Y, eds. Imaging of the wrist and hand. Philadelphia, Pa: Saunders, 1996; 523–546.
5. Hulten O. Über anatomische variationen der hand-gelenkknochen. Acta Radiol 1928; 9:155–169.
6. Epner RA, Bowers WH, Guilford WB. Ulnar variance: the effect of wrist positioning and roentgen filming technique. J Hand Surg [Am] 1982; 7:298–305.
7. Palmer AK, Glisson RR, Werner FW. Ulnar variance determination. J Hand Surg [Am] 1982; 7:376–379.
8. Friedman SL, Palmer AK, Short WH, Levinsohn EM, Halperin LS. The change in ulnar variance with grip. J Hand Surg [Am] 1993; 18:713–716.
9. Tomaino MM. The importance of the pronated grip x-ray view in evaluating ulnar variance. J Hand Surg [Am] 2000; 25:352–357.
10. Loftus JB, Palmer AK. Disorders of the distal radioulnar joint and triangular fibrocartilage complex: an overview. In: Lichtman DM, Alexander AH, eds. The wrist and its disorders. Philadelphia, Pa: Saunders, 1997; 385–414.
11. Palmer AK. Triangular fibrocartilage complex lesions: a classification. J Hand Surg [Am] 1989; 14:594–606.
12. Oneson SR, Scales LM, Timins ME, Erickson SJ, Chamoy L. MR imaging interpretation of the Palmer classification of triangular fibrocartilage complex lesions. RadioGraphics 1996; 16:97–106.
13. Tomaino MM. Ulnar impaction syndrome in the ulnar negative and neutral wrist: diagnosis and pathoanatomy. J Hand Surg [Br] 1998; 23:754–757.
14. Tolat AR, Sanderson PL, De Smet L, Stanley JK. The gymnast's wrist: acquired positive ulnar variance following chronic epiphyseal injury. J Hand Surg [Br] 1992; 17:678–681.
15. Sagerman SD, Zogby RG, Palmer AK, Werner FW, Fortino MD. Relative articular inclination of the distal radioulnar joint: a radiographic study. J Hand Surg [Am] 1995; 20:597–601.
16. Tolat AR, Stanley JK, Trail IA. A cadaveric study of the anatomy and stability of the distal radioulnar joint in the coronal and transverse planes. J Hand Surg [Br] 1996; 21:587–594.
17. Dailey SW, Palmer AK. The role of arthroscopy in the evaluation and treatment of triangular fibrocartilage complex injuries in athletes. Hand Clin 2000; 16:461–476.
18. Deshmukh SC, Shanahan D, Coulthard D. Distal radioulnar joint incongruity after shortening of the ulna. J Hand Surg [Br] 2000; 25:434–438.
19. Feldon P, Terrono AL, Belsky MR. The "wafer" procedure: partial distal ulnar resection. Clin Orthop 1992; 124–129.
20. Loftus JB. Arthroscopic wafer for ulnar impaction syndrome. Tech Hand Upper Extrem Surg 2000; 4:182–188.
21. Hotchkiss RN. Injuries to the interosseous ligament of the forearm. Hand Clin 1994; 10:391–398.
22. Graham TJ, Fischer TJ, Hotchkiss RN, Kleinman WB. Disorders of the forearm axis. Hand Clin 1998; 14:305–316.
23. Bell MJ, Hill RJ, McMurtry RY. Ulnar impingement syndrome. J Bone Joint Surg [Br] 1985; 67: 126–129.
24. McKee MD, Richards RR. Dynamic radio-ulnar convergence after the Darrach procedure. J Bone Joint Surg [Br] 1996; 78:413–418.

25. Lees VC, Scheker LR. The radiological demonstration of dynamic ulnar impingement. J Hand Surg [Br] 1997; 22:448–450.
26. Wolfe SW, Mih AD, Hotchkiss RN, Culp RW, Keifhaber TR, Nagle DJ. Wide excision of the distal ulna: a multicenter case study. J Hand Surg [Am] 1998; 23:222–228.
27. van Schoonhoven J, Fernandez DL, Bowers WH, Herbert TJ. Salvage of failed resection arthroplasties of the distal radioulnar joint using a new ulnar head prosthesis. J Hand Surg [Am] 2000; 25:438–446.
28. Scheker LR. Distal radioulnar prostheses to rescue the so-called salvage procedure. In: Simmen BR, Allieu Y, Lluch A, Stanley J, eds. Hand arthroplasties. London, England: Dunitz, 2000; 151–158.
29. Horii E, Nakamura R, Nakao E, Kato H, Yajima H. Distraction lengthening of the forearm for congenital and developmental problems. J Hand Surg [Br] 2000; 25:15–21.
30. Scheker LR, Severo A. Ulnar shortening for the treatment of early post-traumatic osteoarthritis at the distal radioulnar joint. J Hand Surg [Br] 2001; 26:41–44.
31. Fernandez DL, Capo JT, Gonzalez E. Corrective osteotomy for symptomatic increased ulnar tilt of the distal end of the radius. J Hand Surg [Am] 2001; 26:722–732.
32. Bacorn RW, Kurtzke JF. Colles' fracture: a study of two thousand cases from the New York State Workmen's Compensation Board. J Bone Joint Surg [Am] 1953; 35:643–658.
33. Cooney WP, Dobyns JH, Linscheid RL. Complications of Colles' fractures. J Bone Joint Surg [Am] 1980; 62:613–619.
34. Hauck RM, Skahen J, Palmer AK. Classification and treatment of ulnar styloid nonunion. J Hand Surg [Am] 1996; 21:418–422.
35. Hermansdorfer JD, Kleinman WB. Management of chronic peripheral tears of the triangular fibrocartilage complex. J Hand Surg [Am] 1991; 16:340–346.
36. Topper SM, Wood MB, Ruby LK. Ulnar styloid impaction syndrome. J Hand Surg [Am] 1997; 22:699–704.
37. Biyani A, Mehara A, Bhan S. Morphological variations of the ulnar styloid process. J Hand Surg [Br] 1990; 15:352–354.
38. Garcia-Elias M. Dorsal fractures of the triquetrum: avulsion or compression fractures? J Hand Surg [Am] 1987; 12:266–268.
39. Levy M, Fischel RE, Stern GM, Goldberg I. Chip fractures of the os triquetrum: the mechanism of injury. J Bone Joint Surg [Br] 1979; 61:355–357.
40. Thurston AJ, Stanley JK. Hamato-lunate impingement: an uncommon cause of ulnar-sided wrist pain. Arthroscopy 2000; 16:540–544.
41. Viegas SF, Wagner K, Patterson R, Peterson P. Medial (hamate) facet of the lunate. J Hand Surg [Am] 1990; 15:564–571.
42. Viegas SF, Patterson RM, Hokanson JA, Davis J. Wrist anatomy: incidence, distribution, and correlation of anatomic variations, tears, and arthrosis. J Hand Surg [Am] 1993; 18:463–475.
43. Sagerman SD, Hauck RM, Palmer AK. Lunate morphology: can it be predicted with routine x-ray films? J Hand Surg [Am] 1995; 20:38–41.
44. Nakamura K, Beppu M, Patterson RM, Hanson CA, Hume PJ, Viegas SF. Motion analysis in two dimensions of radial-ulnar deviation of type I versus type II lunates. J Hand Surg [Am] 2000; 25:877–888.
45. Malik AM, Schweitzer ME, Culp RW, Osterman LA, Manton G. MR imaging of the type II lunate bone: frequency, extent, and associated findings. AJR Am J Roentgenol 1999; 173:335–338.

This article meets the criteria for 1.0 credit hour in category 1 of the AMA Physician's Recognition Award. To obtain credit, see accompanying test at http://www.rsna.org/education/rg_cme.html.